The International Journal Of Engineering And Science (IJES)
|| Volume || 4 || Issue || 5 || Pages || PP.01-14 || 2015 ||
ISSN (e): 2319 – 1813 ISSN (p): 2319 – 1805

Recent Developments in Organic Polymers Based- Photovoltaic Cells

Zinzuwadia Mithil, Kothari A Rishabh , Gupta Hansika, Korde Madhulika., Prerna Goswami , M.A.Kerawalla
Institute of Chemical Technology (ICT), Nathala Parekh Marg, Matunga, Mumbai-400 019, India,

ABSTRACT: *In this review article, the uses of organic polymers to make photovoltaic cells have been discussed. The focus is mainly on discussing organic polymer based photovoltaic (OPVs) solar cells, the development of new device technologies and donor polymers that are being researched on. The recent development in this field has led to improved OPV performances with power conversion efficiencies as phenomenal as 9%. However for commercial application of this kind of OPVs, an improved device structure and cost effective processing methods are required. This article reports the polymer design criteria, energy level matching, nano-morphing of polymer/acceptor blend films and local dipole moments of the polymer chains that have been developed in the research that took place over the past 4 years. We emphasize the importance of developing new methods for designing polymers with improved physical properties and development of new technologies to fully understand the fundamentals of OPV mechanisms, which will help improve the power conversion efficiency of the OPV.*

KEYWORDS *- Power Conversion Efficiency, Bulk-heterojuntion, Hybrid Solar Cells, Benzo[1,2-b:4,5-b'] Dithiophene, Fused Dithienogermolodithiophene, Selenium-substituted*

Date of Submission: 11-April-2015 Date of Accepted: 05-May-2015

I. INTRODUCTION

Solar energy proved as a clean, sustainable alternative source to fossil fuels can meet the continuously growing global demands of energy.[1] Solar cells based on the photovoltaic effect are an effective method to convert solar energy into electricity. Today, standard solar panels based on multi-layer single crystalline silicon have achieved power conversion efficiencies of more than 40% which has increased their usage [2] but on the other side, the relatively high cost of the crystalline silicon-based solar panels has led to their depletion of widespread and large scale usage. Therefore, the need of the hour was to find another solar cell technology which can exhibit lower manufacturing costs by utilizing inexpensive and abundant materials. Due to this, polymer solar cells (PSCs) based on organic semiconducting donor and acceptor materials are being pursued by the scientific and industrial communities. Some advantages conveyed by PSCs are that they are relatively cheaper, have tuneable flexibility, have high specific weight, are semi-transparent, get easily integrated into other objects, low environmental impact and allow for scalable material production using various organic synthetic methods and cost-effective roll-to-roll coating and printing techniques.[3-5].

As a good donor material in the PSCs, the conjugated polymer should possess atleast the following three intrinsic features:

i. A broad and strong absorption band providing efficient harvest of solar light available at any given time;

ii. Appropriate highest occupied molecular orbital (HOMO) level and a lowest unoccupied molecular orbital (LUMO) level for establishing efficient charge separation with low energy loss;

iii. High hole mobility which facilitates good charge transport.[6]

In addition to these requirements, they must also be extremely soluble in organic solvents, and when they are blended with (6,6)-phenyl-C61(or C71)- butyric acid methyl ester (PC61BM or PC71BM), bi-continuous networks with nanoscale phase separation should be formed.[7-9] . In order to meet all these specific requirements, structural components in conjugated polymers, including their backbones and side groups, must be designed and modified with utmost care. Continuous research and innovations can reduce the cost of electricity produced by PV (photovoltaic) significantly. The levelized cost of PV electricity was approximately 0.6 €/kWh in Germany in the year 2007 while PV electricity reached the private household price level of approximately 0.25 €/kWh by the end of 2011. Thus solar electricity is gradually reaching the grid parity for private household electricity. Major reduction of costs of PV-modules and inverters have led to this positive development. But according to the EIA Annual Energy Outlook 2011 hydro-, coal- or gas-powered plants can

produce electricity well below 0.1 €/kWh. This means that, for making a significant contribution to the global electricity or energy production, the costs for solar electricity still needs to undergo substantial further cost reductions.
Thus cheaper PV-electricity can be achieved in two ways :-

(i)By increasing the power conversion efficiency maintaining PV-material costs the same (wafer-based solar cells (1st generation) or high efficiency concepts (3rd generation)).

(ii)Or by developing low-cost, moderate efficiency PV-material (thin-film PV, organic photovoltaic).

Thus three main contributors can be identified on analysing the typical cost structure of a grid connected PV-system:

(i)PV module,

(ii)Installation/balance of system and

(iii)Power electronics (inverter).

Thus for PSCs to fully develop from research and development to cost effective products, continuous improvement in solar cell efficiency needs to be carried on. A PCE (Power conversion efficiency) of 10% or more in devices with sizable area is regarded as an important threshold for practical and widespread usages of polymer solar cells. It has been found out that PSCs showing 15% PCE with a 20-year lifetime can provide electricity at a cost of around seven cents per kilowatt-hour which makes solar energy competitive with conventional sources of electricity.[10-11] And thus for achieving this PCE goal, major advances in new materials and device technology is highly essential. [12-13]

II. BULK HETEROJUNCTION (BHJ) SOLAR CELLS

The most popular class of PSCs , the bulk heterojunction (BHJ) solar cells are based on composite materials composed of low band-gap conjugated polymers as the electron donor, and substituted fullerenes as electron acceptor materials. Due to successive developments in material design and synthesis, control in the morphology of the bulk heterojunction (BHJ) composite and device optimization, power conversion efficiencies (PCEs) of more than 8% have been achieved.[14-23] Efficiency approaching 10% has been disclosed in small area solar cells, which indicates the rapid progress over the last 5 years and the great potential of these polymer solar cells as an alternative source of energy.[24]

Detailed balance limit and charge transfer complex

Veldman et al. [25] conducted a number of experiments on the charge transfer complex in bulk heterojunction and found out that the minimum open circuit loss amounts to 0.6 eV unlike the lower band gap of the acceptor and the donor. The open circuit voltage(V_{oc}) and the HOMO–LUMO difference of the donor acceptor pair as well as the V_{oc} and the energetic position of the charge transfer complex emission showed a linear relation. Now they used this relation and assumed values for the External Quantum efficiencies (EQE) and the fill factors (FF) to calculate the ultimate efficiency of BHJ cells. With a FF and EQE of about 65% they found a maximum efficiency of 11% which was obtained at a band gap around 1.4 eV. This highlights the importance of the charge transfer complex formed in organic solar cells.[26]

Fig 1.Illustration of the different losses in an perfect solar cell, photon energy larger or smaller the absorber gap (left); power conversion efficiency losses according to the Shockley–Queisser analysis. _E1is the photon access energy which is lost due to fast relaxation of the photoexcited charge carrier. Photons with energy E2smaller than the band gap are not absorbed by the semiconductor.

In 2009 Kirchartz et al.[27] calculated the radiative efficiency limit of organic solar cells. Adapting the Shockely–Queisser approach(above figure) they estimated a maximum efficiency >20% for pristine polymer and polymer fullerene absorbers. The analysis showed a power conversion efficiency of max. 4.2%, which was investigated upon and the following losses were revealed:

1. Optical losses.

2. Exciton losses due to insufficient transport of excitons to the next donor– acceptor interface or due to

inefficient exciton dissociation.

3. Non-radiative recombination losses.
4. Charge carrier collection losses due to insufficient mobilities.

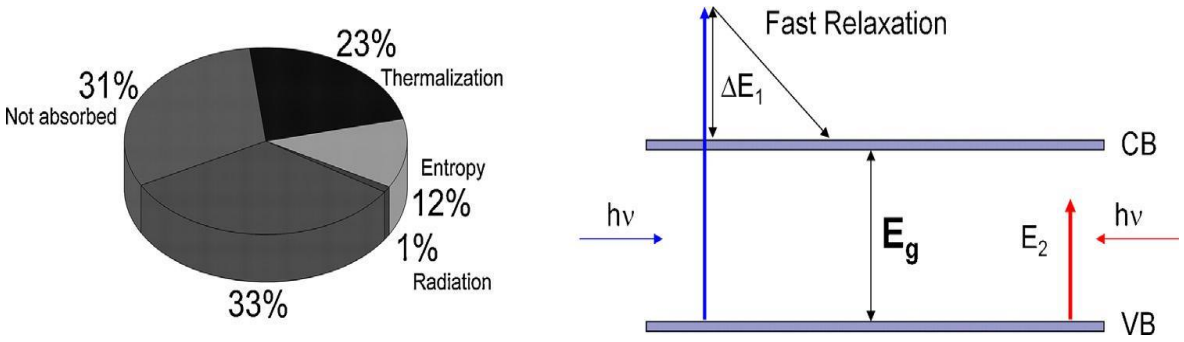

To overcome the non-radioactive recombination losses, the morphology of the BHJ films was required to be appropriate [28] so that excitons can be created within a diffusion length of a donor-acceptor interface, leading to greatly enhanced quantum efficiency of charge separation.

Yu and co-workers [15,29,30] reported a series of examples of donor 95 copolymers incorporating TT and benzo (1,2-b;4,5-b') dithiophene (BDT) (PTBs). The planarity of the BDT molecule with an extended π conjugated system conveys rigidity to the polymer backbone, enabling the polymer to form an assembly with better π–π stacking and high hole mobility. This improves the hole mobility and hence reduces the losses.

Recently Koster et al.[31]and Gruber et al.[32] pointed out that either a very weakly absorbing or a strongly absorbing charge transfer state leads to the highest power conversion efficiencies under the radiative efficiency limit. A weakly absorbing CT minimizes the losses in open circuit voltage while a strongly absorbing charge transfer state allows the collection of additional photons(solar). In both cases, the maximum efficiency in the radiative limit is

above 30%. The situation is illustrated in below fig. Here we assume a charge

transfer state with different absorptions strength with a constant spectral width of 0.2 eV. They performed the calculations using a black body radiator with a surface temperature of 5800 K as source of light and intensity at the solar cell surface of 1000 W/m^2 and a solar cell temperature of 300 K.

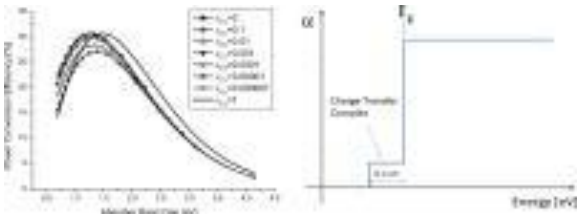

Fig 2.(a) Profile of an ideal absorber with a weak and broad charge(0.2 eV) transfer absorption feature. (b) PCE of a solar cell with a absorption profile (a) and different absorptions strength (CT) of the charge transfer state

Giebink et al.[33] found a "Thermodynamic Efficiency Limit of Exciton Solar Cells" of

22–27%—demonstrating again the performance potential of organic solar cells under idealized conditions without any losses. Similarly high efficiencies for bulk heterojunction solar cells can be found out by applying pure thermodynamic considerations.

III. ORGANIC—INORGANIC HYBRID SOLAR CELLS

Organic—inorganic hybrid solar cells combine inorganic nano particles and organic (normally conjugated polymers), with the intent of using the advantages associated with both material groups [34,35]. The device fabrication and operation of hybrid solar cells is very similar to that of organic solar cells, the only difference being that the organic electron accepting material of PCBM (or other fullerene derivatives) is replaced by an inorganic nanoparticle. The inorganic electron acceptor material provides many advantages to the system, whilst maintaining low cost process ability.

First of all inorganic materials are more environmentally stable than organic materials [36]. Adding these materials to OPV devices assists in overcoming one of the major downfalls of this technology, ie the photo induced degradation of the conjugated organic semiconductors. Second, photogeneration of charge carriers is achieved by excitons absorbed in the inorganic material [37,38]. Also the contribution of light absorption by an inorganic acceptor is potentially greater than the absorption contribution of PCBM in PSC devices [39,40].
Finally, inorganic quantum dots are also known for ultrafast photoinduced charge carrier transfer to organic semiconductors. This transfer rate has been observed and calculated in the order of picoseconds [41]. As this transfer rate is faster than the competing recombination mechanisms ,efficient charge transfer is established between the donor and acceptor .

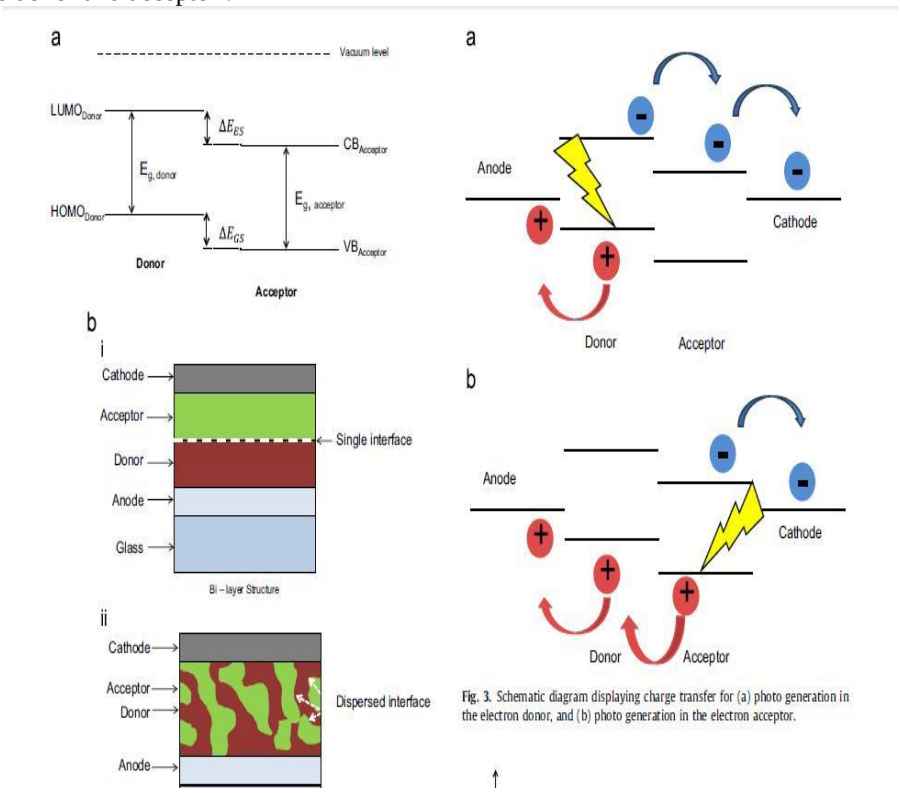

Fig. 3. Schematic diagram displaying charge transfer for (a) photo generation in the electron donor, and (b) photo generation in the electron acceptor.

Device operation

The exciton created on the absorption of a photon is dissociated at the donor-acceptor interface. When they separate, the electron is transfered to the acceptor material at an interface and travels to the cathode for charge collection. The hole produced in the donor material is collected at the anode after travelling throughout the polymer. This process is displayed as (a) in Fig. When light is absorbed in the acceptor material, an exciton is formed which must be dissociated by the offset in energy of the donor HOMO level and the acceptor valence band edge. The hole is transferred to the donor at an interface and reaches the anode whilst the electron remains in the acceptor material and travels to the cathode for collection. This process is displayed as (b) in above Fig. Various design considerations are crucial while choosing an appropriate inorganic material. It has been identified that an optimal electronic design for such a material would be a bandgap of 1.5eV and a HOMO level offset of 0.3eV so that it allows both a significant absorption contribution as well as a large open circuit voltage (Voc). There exist additional physical considerations which must also be taken into account. The different materials which have so far been considered have both advantages and disadvantages; however, none of materials has been coupled with a polymer to provide an electrical performance superior to that of an OPV device, for which PCEs of 10% have been achieved. The major limitation to device performance is due to the

effect of the insulating surface ligand on the electrical performance of the nanoparticles. Recent research aim at realizing the entire potential of this technology by reducing the negative effects.[42] Silicon is a good choice for nanohybrid solar cells and it has higher dielectric constant as compared to PCBM. It has strong electronic properties which is desirable for us. Lie et al studies this and found the bandgap of Si N Cs, to be 1.5eV.Due to the relatively small bandgap, they provided an enhanced absorption profile. The absorption profile of P3HT:PCBM is compared with that of Si NCs in figure

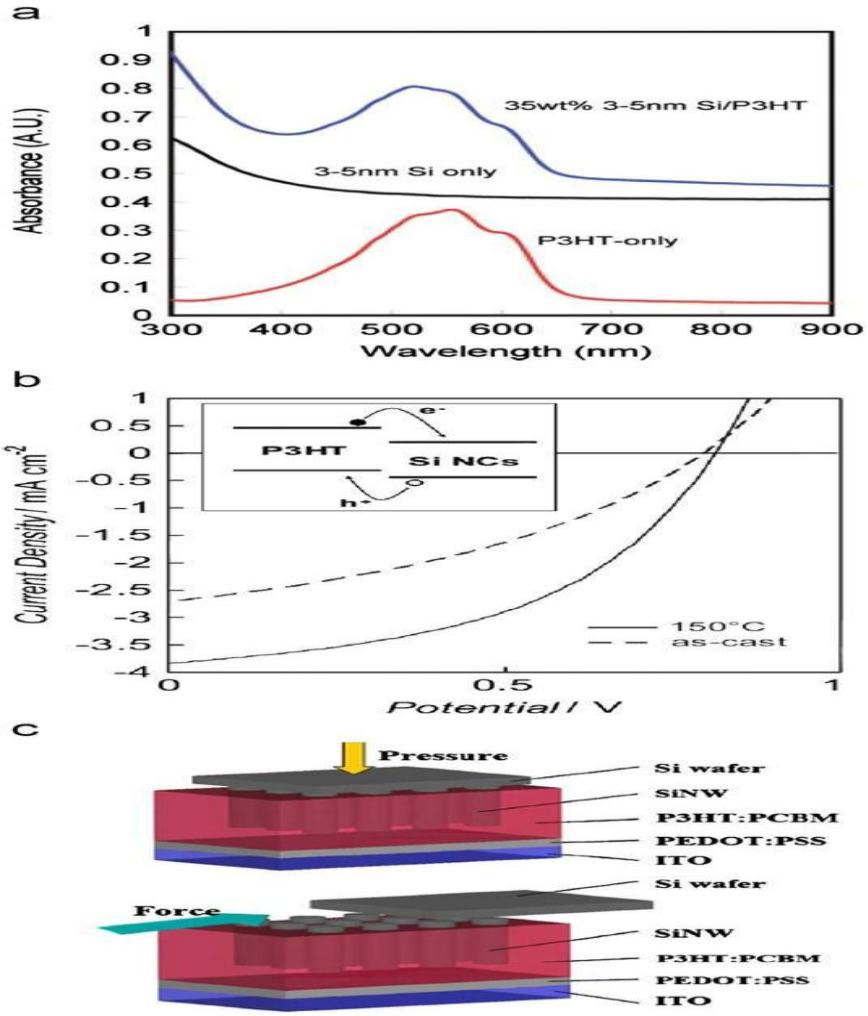

Fig 4. Optical absorption spectra forP3HT, silicon nanocrystals and P3HT:Si NC blendfilm [88], (b) J–V characteristic curves of P3HT:SiNCsolar cells under 100 mW/cm2, AM1.5G conditions. This shows a comparison of an as-cast and annealed device. The annealing conditions were 150 C for 120min ,Schematic diagram of the procedure used to form hybrid solar cells incorporating silicon nanowires. First, the nanowires were pressed into the P3HT:PCBM blend, then the wafer was removed by the application of lateral force

Scharber et al in 2006 studied the relationship between the open circuit voltage and the energy levels of the D-A blend for 26 different BHJ devices. Keeping the acceptor(PCBM) constant, the donor material was varied.[43,44] The analysis suggested linear relationship between the open circuit voltage and the diagonal bandgap of the heterojunction but there also existed a loss factor in the BHJ design.

However there are problems related to the increased density of trapped states and limited control over the D-A nanomorphology which seemed to have hindered progress in this field. However, a post production annealing process could improve the nanomorphology and hence improve the PCE. Thermal treatments cause crystallinity in the polymer hence allowing better hole mobility [45-47].Similarly, many ways of nanostructuring are possible which improve the electron mobility in the polymer(below Fig.).Inorganic materials like semiconductor ZnO have come to the limelight due to their vertically aligned structures and high electron nobilities. Hence, many new materials were explored to work towards optimizing such parameters.

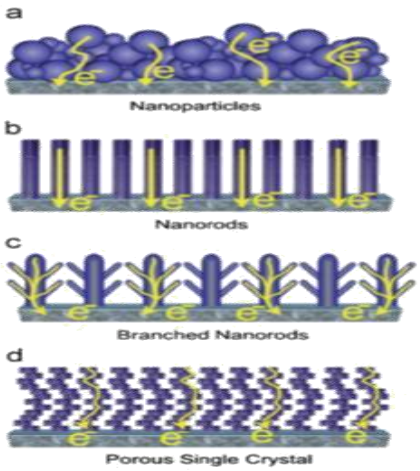

Fig5. Schematic representation of the possible nanostructured architectures for inorganic acceptor materials. Depicted are (a) quantum dots, (b) nano rods, (c) branched nano rods and (d) porous single crystal.

IV. FROM ALKOXY-SUBSTITUTED BENZO[1,2-B:4,5-B′]DITHIOPHENE UNITS (BDT) TO

2-Alkylthienyl-Substituted BDT

Table 1. Properties and Photovoltaic Results of Three Pairs of BDT-Based Polymers with Alkoxyl Substitution and 2-Alkylthienyl Substitution

	properties of the polymers				photovoltaic data of the corresponding PSCs					
material	λ_{edge} [nm]	E_g^{opt} [eV]	HOMO [eV]	T_d [°C]	V_{oc} [V]	J_{sc} [mA/cm^2]	FF [%]	PCE [%]	μ_h [cm^2/(Vs)]	ref
PBDTTT-C-O	776	1.60	−5.07	320	0.70	15.51	59.2	6.43	5.53×10^{-4}	33
PBDTTT-C-T	788	1.58	−5.11	428	0.74	17.48	58.7	7.59	0.27	33
PBDTDTQx-O	714	1.74	−5.12	320	0.71	7.00	61.5	3.06	4×10^{-5}	34
PBDTDTQx-T	740	1.67	−5.12	430	0.76	10.13	64.3	5.00	1.04×10^{-4}	34
PBDPP-O	880	1.45	−5.29	330	0.69	6.50	63	2.83	4.48×10^{-2}	35
									2.45×10^{-2}	35

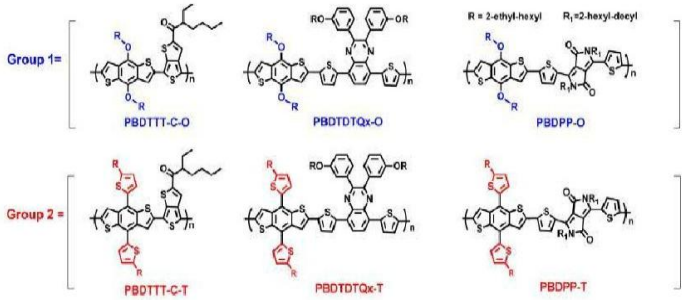

BDT based polymers are one of the major families of polymer based photovoltaic cells.[48-60] After studying the reported works on these PVCs, it has been found that efficient photovoltaic materials can be obtained by copolymerizing BDT units with other types of conjugated building blocks.[48] Thus, 8−9% PCEs have been obtained from BDT and Thieno(3,4-b) Thiophene (TT) Copolymers, [53-58] the BDT andTPD copolymers,[59] the BDT and diketopyrrolopyrrole (DPP) copolymers,[60,61] and so on. Therefore, how to improve photovoltaic properties of the BDT-based polymers is a very important topic for molecular engineering and thus further research needs to be carried on.

4.1 Design strategies of the 2D-conjugate BDT based polymers

In the above figure, there are two groups in which six BDT-based polymers are put in. In Group 1, the BDT units in the polymers are substituted by alkoxyl groups; in Group 2, the backbone structures of the three polymers are identical and possess alkyl side groups as the analogues of Group 1, but the

Fig 6.evolution of moleculer structures based structures for three BDT based polymers from alkoxyl substitution to 2-alkylthienyl substitution

Alkoxyl groups linked with the BDT units are replaced by 2-alkylthienyl groups, so that the surface area of conjugation of their backbones can be expanded toward the vertical direction. The comparisons between the polymers in these two groups will provide further important information on the effects of the 2D-conjugated structure.[62,64] According to the data collected in Table 1, it can be concluded that due to the replacement of the alkoxyl groups with the 2-alkylthienyl groups, the absorption bands of the polymers get red-shifted slightly, while their HOMO levels are little altered. Also, the thermal decomposition temperatures (Td) of the polymers in Group 2 are improved by quite an extent. In addition to that, the polymers in Group 2 showed higher hole mobility and improved PCEs in PSCs compared to the polymers in Group 1.

Table 2. Band Gaps and HOMO Levels of the BDT-Based Polymers with Different Conjugated Side Groups and the Corresponding Photovoltaic Results

material	E_g^{opt} [eV]	HOMO level [eV]	V_{oc} [V]	J_{sc} [mA/cm^2]	FF [%]	PCE [%]	ref
PBDTDPP-O	1.31	−5.16	0.68	8.4	44.3	2.53	36
PBDTDPP-T	1.44	−5.30	0.73	14.0	65	6.6	14
PBDTDPP-P	1.46	−5.35	0.76	13.6	60	6.2	14
PBDTDTBT-O	1.72	−5.24	0.79	13.56	69.1	7.40	38
PBDTDTBT-P	1.70	−5.35	0.88	12.94	70.9	8.07	37
PBT-T	1.67	−4.95	0.60	13.7	67.7	5.6	40
PBT-OP	1.70	−5.17	0.78	13.4	71.8	7.5	40
PBT-0F	1.61	−4.90	0.56	12.2	66.7	4.5	22
PBT-2F	1.64	5.15	0.74	14.4	67.7	7.2	22
PBT-1F	1.65	−4.95	0.60	14.3	65.7	5.6	22
PBT-3F	1.64	−5.20	0.78	15.2	72.4	8.6	22

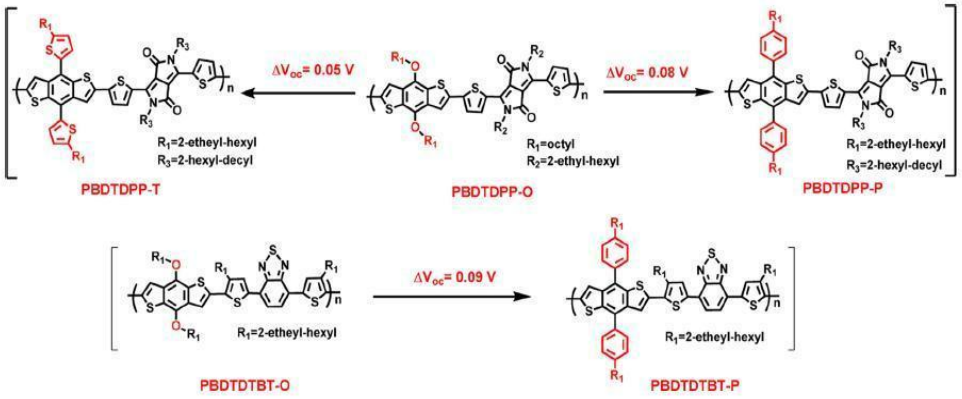

4.2. Molecular Energy Level Modulation of the 2D-Conjugated BDT-Based Polymers

Recent studies in the molecular designs of 2D-conjugated BDT-based polymers showed that molecular energy levels of this type of polymers can be tuned effectively by altering the conjugated side groups.
Figure - Evolution of molecular structures for BDT-based polymers with different conjugated side groups.
Right from alkoxyl substitution to 2-alkylthienyl substitution, little change in their HOMO levels are observed, meaning both the 2-alkylthienyl groups and the alkoxyl groups have similar influence on molecular energy levels of the BDT-based polymers. Yang et al. synthesized two

Fig 7. Evolution of molecular structures for BDT-based polymers with different conjugated side groups.
copolymers namely BDT and DPP [61] in which thienyls and phenyls were respectively used as the conjugated side groups.

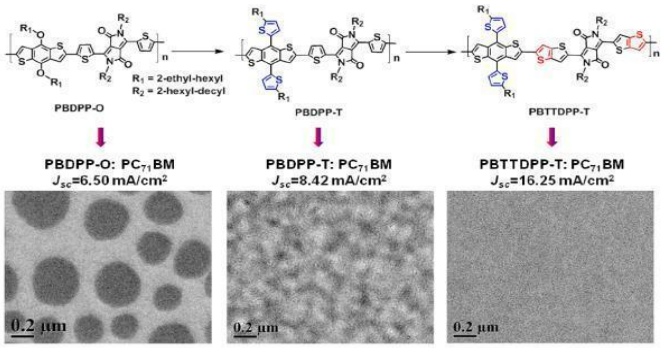

To enable clear comparisons, the analogous polymers based on alkoxyl-substituted BDT36 are shown in above Figure , and each of their photovoltaic properties is collected in Table 2. The figure shows the TEM images of the corresponding polymer:PC71BM blends significantly and the molecular structures of three polymers based on the BDT and DPP units. The substituent's on BDT were changed from alkoxyl to 2-alkylthienyl and then to para-alkylphenyl, their HOMO levels decreased gradually, from −5.16 to −5.30 eV and then to−5.35 eV; while the Voc's of the corresponding PSCs got increased from 0.68 to 0.73 V and then to 0.76 V. Thus molecular energy level of the 2D-conjugated BDT-based polymers is also affected by altering the substitution positions of the alkyls.[65] Recently, Huang et al. did a detailed study on the effect of alkyl substitution position on molecular energy levels of the 2Dconjugated BDT-based polymers and noticed a PCE of 7.1% with a high Voc of 0.9 V.[66] The molecular energy levels can also be tuned by introducing functional groups onto their conjugated side groups. In a previous work, when meta-alkoxyl-phenyl was used as side groups instead of para-alkoxyl-phenyl in a conjugated polymer, deeper HOMO level and thus improved Voc was noticed.

Fig 8. Molecular structures of three polymers based on BDT and DPP units, and TEM images of the corresponding polymer:PC71BM blends.

Based on the discussion in this section it should be concluded that molecular energy levels of the 2D-conjugated BDT-based polymers can be effectively tuned according to the requirements.

4.3. Backbone Conformation Modulation of the2D-Conjugated BDT-Based Polymers

Getting bicontinuous nanoscale phase separation in the blends of polymer and PC71BM (an electron acceptor) is one of the key issues to ensure efficient PCE. Sometimes, the formation of large size aggregations of polymer and PC71BM in the blends is one of the most important obstacles in order to realize high photovoltaic performance.As shown in Figure , the PBDPPO:PC71BM blend showed large aggregations (>100 nm), so that the excitons generated in the polymer and PC71BM domains cannot diffuse to the D/A interface efficiently due to the limited exciton diffusion length and also the D/A interface in the blend is not big enough to perform efficient charge separation. Although the replacement of the alkoxyls with the 2- alkylthienyls definitely have a positive influence on improving compatibility between PCBM and the polymer based on DPP and BDT,[64]this method doesn't have much of an effect on tuning crystallinities of the BDT-based polymers.[67,70] From the results discussed above it can finally be concluded that morphological properties of the 2D-conjugated BDT-based polymers can be tuned by a variety of methods. The superior properties of 2D-conjugated BDT-based polymers along with high PCEs make them potential candidates for highly efficient photovoltaic solar cell devices with varied architectures. The molecular structure evolutions from BDT to 2D-conjugated BDT is an excellent reference for the design and development of organic-polymer electronic materials. These excellent results indicate that 2D-conjugated BDT is a very useful building block for the design of high performance photovoltaic polymer solar cells.[71]

V. FUSED DITHIENOGERMOLODITHI- -OP HENCE LOW BAND GAP POLYMERS

Another promising class of polymers for the photovoltaic applications are the so-called ladder polymers, in which linked aromatic units such as thiophene or benzene are forced to be co-planar and fully conjugated using the bridge heteroatoms.[72] The enforced co-planarity reduces rotational disorder which leads to lowering of reorganization energy and potentially increasing charge carrier mobility.[73] The bridging atoms also serve as a point of attachment for the necessary solubilizing groups needed to ensure processable materials. Thus here we have dithienogermolodithiophene which is the polymer in which two thieno(3,2-b)thiophene units are held co-planar by a bridging dialkyl germanium is polymerized with with *N*-octylthienopyrrolodione by Stille polycondensation giving a polymer, **pDTTG-TPD**, which has an optical band gap of around 1.75 eV and is combined with a high ionization potential. BHJ solar cells based upon **pDTTG-TPD**:PC71BM blends afforded efficiencies up to 7.2% without the need for thermal annealing or processing additives.

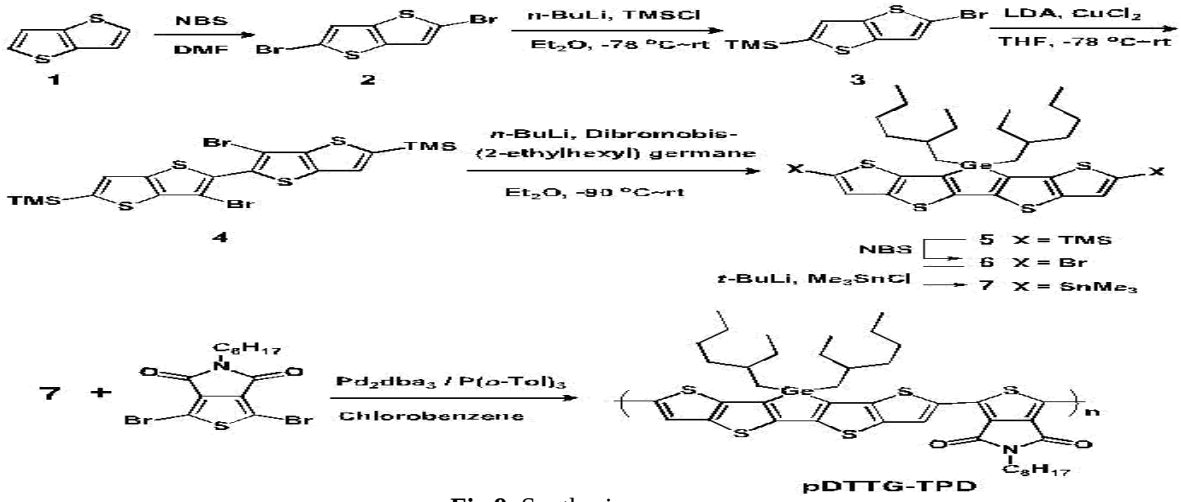

Fig 9. Synthesis process

The synthesis of the polymer **pDTTG-TPD** is shown in scheme 1. Dibromination of commercially available **TT** with NBS, followed by protection of one of the aryl bromides as a trimethylsilyl group resulted from the previously reported **TT** derivation **3**. In this method we use the property of arylhalides to undergo base catalyzed rearrangements (the halogen dance mechanism) to produce the most stable organometallic species. The treatment of 5-bromothieno[3,2-b]thiophen-2-yl) (trimethyl) silane **3** with one equivalent of LDA at -78°C Resulted in the rearranged 6-bromothieno[3,2-b]thiophen-2 yl) (trimethyl)silane. This was not isolated, but was oxidatively dimerised *in situ* by treatment with $CuCl_2$ to produce the dibromide **4** in 70%. This was dilithiated at - 90°C and reacted with dibromobis (2-ethylhexyl) germane to afford the ring closed germole **5** in 60%. Note that the di-anion of **4** had a tendency to decompose by ring opening due to the electron rich nature of the thieno[3,2-b]thiophene. This degradation could be minimized by maintaining the temperature below - 90°C, and using diethyl ether rather than THF as the solvent. The conversion to the required distannyl derivative of germole **5** was achieved by treatment with NBS, followed by lithiation of the resulting dibromide and stannylation at low temperature.[74] The optical properties of **pDTTG-TPD** were characterized by UV-vis absorption spectroscopy. As shown in below Figure , the solution spectrum displays a maximum at 595 nm and a shoulder at 643 nm. The shoulder is assigned to the aggregation of **pDTTG-TPD** since heating to 85 °C results in a 7 nm blue shift of the maximum and a decline in the relative intensity of the shoulder. This suggests the existence of inter-molecular stacking even in dilute solution. Upon film formation the absorption red shifts and the relative peak intensities change, with the former shoulder now becoming the strongest intensity peak at 663 nm with a weaker shoulder at 608 nm. Such changes are indicative of an increasing degree of polymer aggregation and backbone planarization com-pared to solution. From the onset absorption in the solid state, the optical band gap was found to be approximately 1.75 eV.

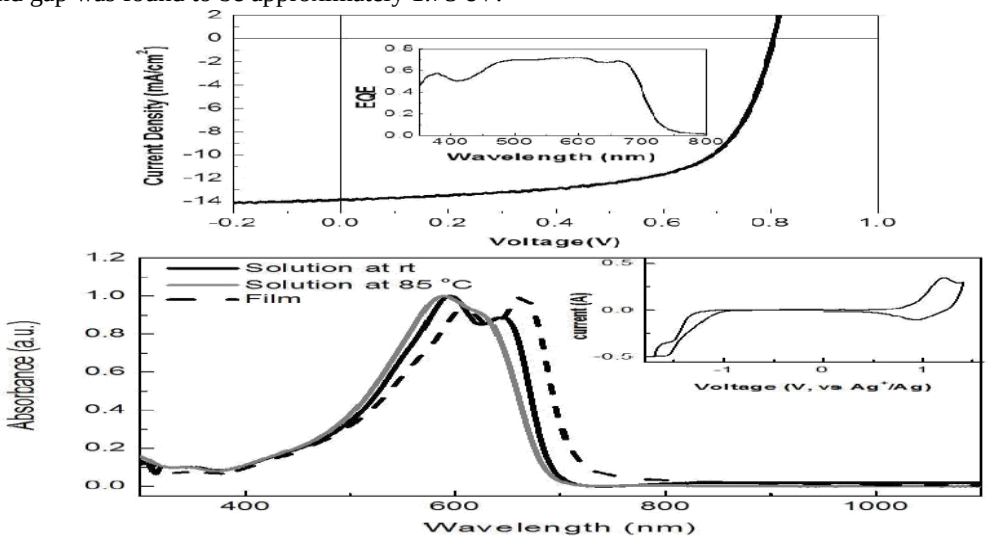

Fig 10. Absorption of **pDTTG-TPD** in chlorobenzene and of **pDTTG-TPD** in 0.1 M Bu_4NPF_6 acetonitrile solution.

In order to calculate the band gap and energy level of **pDTTG-TPD** we measured the redox behavior by cyclic voltammetry (CV) as a thin film. The inserted curve in Figure shows that **pDTTG-TPD** possesses a reversible oxidation and an irreversible reduction. Based on the assumption that the absolute energy level of ferrocene/ferrocenium (Fc / Fc^{+}) is -5.1 eV to vacuum [75], the energy levels of the highest occupied molecular orbital (HOMO) and lowest unoccupied molecular orbital (LUMO) were evaluated with the value of - 5.68 eV according to their oxidation onset potentials and according to their reduction onset potentials the value was -3.88 eV. As a result the value of electrochemical band gap was calculated as 1.8 eV, which is in excellent agreement with that of optical band gap.

The photovoltaic performance of **pDTTG-TPD** was investigated in bulk heterojunction devices with a conventional device configuration of ITO/PEDOT:PSS/PTTGTPD:PC71BM/Ca/ Al. The best device performance based on the film spin-coated from an optimal 1:2 (w/w) ratio of p**DTTG-TPD**/PC71BM blend solution in dichlorobenzene at 80 °C can be seen in the above figure. Further annealing at 140 °C did not change the performance. The optimum active layer thickness was found to be between 90-110 nm, limited by the limited solubility of the donor polymer. The illuminated (A.M. 1.5) current density-voltage (*J-V*) curve in figure 2 exhibits a V_{oc} of 0.81 V, a J_{sc} of 13.85 mA cm^{-2} and a FF 0f 64%, leading a PCE of 7.2%. Average device efficiencies were 6.8% . This good performance was achieved without the use of any processing additives. Such additives are often required in the case of largely amorphous donor polymers to drive phase segregation during the film drying process by preferential solubility of one of the components in the additive.

VI. A SELENIUM-SUBSTITUTED LOW-BANDGAP POLYMER

The reduction of the band gap and the enhancement of the charge transport properties of a LBG (low bandgap polymer) polymer (PBDTT-DPP) can be accomplished simultaneously by substituting the sulfur atoms on the DPP (diketopyrrolopyrrole) unit with selenium atoms. The newly designed polymer,benzo[1,2-b;3,4-b]dithiophene-alt-2,5-bis(2-butyloctyl)-3,6-bis(selenophene-2-yl)pyrrolo[3,4-c]pyrrole-1,4-dione} (PBDTT-SeDPP, Eg = 1.38 eV), shows excellent photovoltaic performance in single junction devices with photo-response up to 900 nm and PCEs over 7%. Visibly-transparent solar cells and tandem polymer solar cells and based on PBDTT-SeDPP are also demonstrated with a 9.5% and 4.5% PCE, which are more than 10% enhancement over those based on PBDTT-DPP

The SeDPP monomer was synthesized by first adding the carbonitrile group onto the 2-position of selenophene. The SeDPP core unit was formed by condensation reaction with selenophene-2-carbonnitrile and diisopropylsuccinate in a basic environment. It should be noted that decreasing the reaction temperature (from 120 C to 80 C) and increasing the reaction time (from 2 hours to 12 hours) can enhance the yield of this step to a great extent, probably due to the lack in stability of the selenothiophene-2-carbonnitrile at high temperature. Then, 2-butyloctyl chains were attached onto the DPP core to ensure it was soluble and then finally the bromination was performed by N-bromosuccinimide (NBS) under Argon protection. To fully measure the effect of the Se-substitution on the DPP unit, the furan and thiophene counterparts (PBDTT-FDPP and PBDTT-DPP) were also synthesized and characterized for comparison, and their chemical structures are shown in **Figure** a. The polymers PBDT-FDPP, PBDTT-DPP, and PBDTT-SeDPP were obtained via Stille-coupling polymerization, and the detailed synthetic route as well as structural characterization is described in the Supporting Information. The gel permeation chromatography (GPC) measurements measures similar average molecular weights (M_n) of 35.2 kDa, 40.7 kDa, and 38.4 kDa for PBDTT-FDPP, PBDTT-DPP, and PBDTT-SeDPP, respectively. It is seen that higher M_n batches of PBDTT-DPP and PBDTT-SeDPP showed very poor solubility and cannot be used for solution processing. And higher M_n batches of PBDTT-FDPP showed similar or even lower performance. For the consistency of the report, polymers with similar M_n values are used here. The polydispersity index of these three polymers was also determined by GPC to be around 2.1. These polymers can be dissolved in chloroform (CF), chlorobenzene (CB), and dichlo-robenzene (DCB).

Figure b shows the comparison of the ultraviolet/visible (UV/Vis) absorption spectra of the polymer thin films. All three polymers have a main absorption range starting from ~550 nm, and the absorption edges are from 810 nm to 900 nm. The absorption shapes are similar to each other, which indicate the characteristics of the BDTT-DPP backbone system. The new PBDTT-SeDPP polymer displays a clear red-shift of the absorption onset as well as the maximum peak value (nearly 50 nm) as compared to PBDTT-DPP. According to the onset of the film absorption spectra, the optical band gap of PBDTT-DPP, PBDT-FDPP and PBDTT-SeDPP are calculated to be 1.46, 1.51 and 1.38 eV, respectively. The relatively low absorptivity in the visible region (400–650 nm) and high absorptivity in the NIR (650–900 nm) and UV (<400 nm) region of PBDTT-SeDPP make it a very promising candidate for high performance tandem PSCs and visibly-transparent PSC applications.[76]

Fig 11. (a) Chemical structures of PBDTT-FDPP, PBDTT-DPP and PBDTT-SeDPP,

(b) Absorption spectra in thin films of PBDTT-FDPP, PBDTT-DPP and PBDTT-SeDPP.

It was seen that by substituting the sulfur atoms with selenium atoms, the HOMO level increases slightly and meanwhile the LUMO level drops a little. The narrowing of the bandgap is mainly due to the electron stabilizing effect of selenophene moieties, since selenium is more polarizable than either sulfur or oxygen.[77,78] The actual HOMO and LUMO energy levels of polymers are then determined by cyclic voltammetry (CV) measurement and the results from both DFT calculation and CV measurements are summarized in the given table. The HOMO/LUMO levels of PBDTT-FDPP, PBDTT-DPP, and PBDTT-SeDPP are measured to be −5.26/−3.64 eV, −5.30/−3.63 eV, and −5.25/−3.70 eV, respectively. The bandgap of PBDTT-FDPP turns out to be the smallest based on the CV testing, which conflicts with the optical bandgap

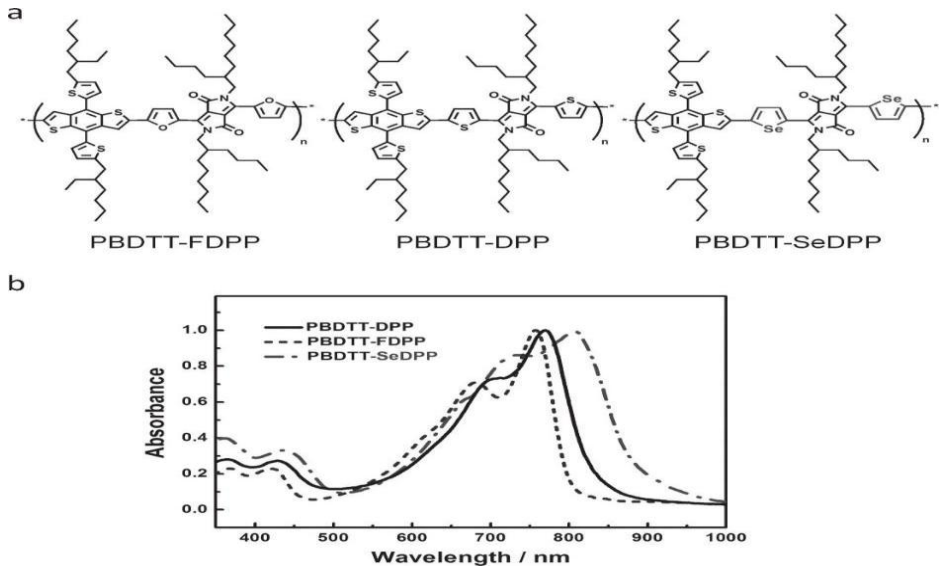

Single junction BHJ solar cell performance of these polymers were preliminarily investigated with the regular structure of ITO/PEDOT:PSS (30 nm)/polymer:PC71BM (100 nm)/ Ca/Al under AM1.5G illumination (100 mW/cm^2). These three polymers were spin-coated onto the PEDOT:PSS coated indium-doped tin oxide (ITO) glass substrate from DCB solution, followed by the evaporation of Ca/Al as top electrode. The optimized polymer:PCBM ratio was found to be 1:2 by weight. Typical current density-voltage (J-V) curves are shown in **Figure** , the corresponding EQE(external quantum efficiency) curves are presented in Figure 2b and the results are summarized in **Table 3**

Table 3. Photovoltaic properties of single layer BHJ solar cells.

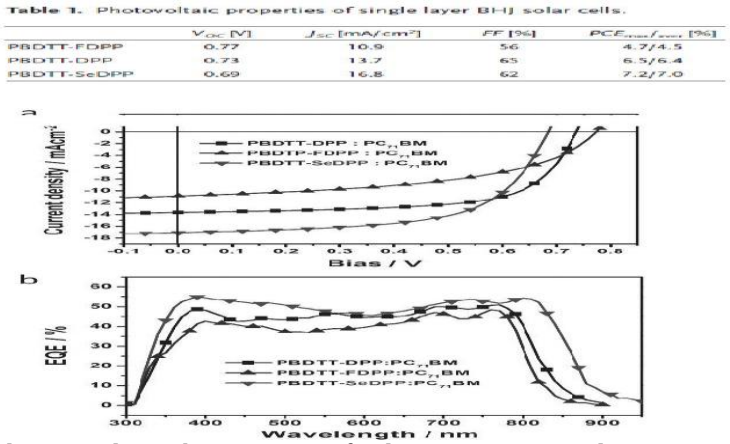

Fig 12.(a) Current density-voltage characteristics of polymer/$PC_{71}BM$ single junction solar cellsunder AM1.5G illumination (100 mW/cm^2).
(b) EQEs of the corresponding devices

The PBDTT-SeDPP based device turns out to have the lowest V_{OC}, and it is mainly due to a relatively high HOMO energy level. The J_{SC}, increases from PBDTT-FDPP to PBDTT-DPP to PBDTT-SeDPP based devices. A high *JSC* of 16.8 mA/cm^2 was observed in PBDTT-SeDPP based devices, which is 52% and 23% higher than PBDTT-FDPP (10.9 mA/cm ^{2}) and PBDTT-DPP (13.7 mA/cm^2) based devices. With an *FF* of around 62%, the PBDTT-SeDPP based device shows a maximum efficiency of 7.2% (the averaged PCE from ~40 devices is 7.0%), whereas the PBDTT-FDPP and PBDTT-DPP based devices show max/average PCEs of 4.7/4.5% and 6.5/6.4%, respectively. From the EQE results (Figure 2b), a broader coverage of PBDT-SeDPP from 300 nm to 900 nm is clearly seen. Also, the average values (note: estimated from numerical values between the two peaks at ~350 and ~800 nm) are around 42%, 47% and 53% for PBDTT-FDPP, PBDTT-DPP, and PBDTT-SeDPP based single-layer devices, respectively. It was seen that the maximum EQE for the LBG polymers (~50%) are still lower than the state-of-art MBG polymers such as PTB7 (~60%).The IQE(internal quantum efficiency) of PBDTT-SeDPP based devices was around 60%, indicating there is still significant energy loss during the photon-to-electron conversion process.

VII. CONCLUSION

Over the past four years, OPVs have made rapid progress and its PCE has exceeded 10%. With the development of many new donor polymers such as Bulk heterojunction (BHJ) solar cells (8-10%), Organic—inorganic hybrid solar cells (approx 10%), Alkoxy-Substituted benzo[1,2-b:4,5-b′]dithiophene units (BDT) to 2-Alkylthienyl-Substituted BDT (8-10%), Fused Dithienogermolodithiophene low band gap polymers (7-8%) and Selenium-Substituted Low-Bandgap Polymer (8-9%) higher PCE can be achieved. Also, further new criteria has been established to consider a polymer as donor polymer, such as satisfying a broad absorption with a high extinction coefficient near the region of maximum solar photon flux, a low lying HOMO energy level and a suitable LUMO energy level. Also, it is important that the polymer has appropriate miscibility with n-type acceptor materials. When the polymer satisfies these physical properties, the local dipole moment along the polymer chain is critical for effective exciton separations and charge carrier generation. Apart from the characteristics of the polymer required for high solar cell efficiency, the polymer's photochemical stability and the stability of donor/acceptor's nano-morphology are crucial issues towards achieving longer lifetimes. In addition to development of high efficiency materials, technologies must also be developed for fabricating reasonable, lightweight and flexible devices which show the device's lifetime suitable for commercialization. In our view, the perspective for OPVs is very bright and is becoming brighter as the years go by.Thus Cheap Enviorenmental Friendly Solar Energy is a key to a healthier and bright future.

REFERENCES

[1]. F. C. Krebs, Polymer Photovoltaics A Practical Approach; SPIE Press, Bellingham, 2008.
[2]. M. A. Green, K. Emery, Y. Hishikawa, W. Warta, E. D. Dunlop, Prog. Photovoltaics, 2011, **19**, 565−572.
[3]. B. C. Thompson, J. M. J. Frechet, Angew. Chem., Int. Ed., 2008, 100 **47**, 58–77.
[4]. S. Gunes, H. Neugebauer and N. S. Sariciftci, Chem. Rev., 2007, **107**, 1324-1338.
[5]. H. Spangaard and F. Krebs, Sol. Energy Mater. Sol. Cells., 2004, **83**, 125-146.
[6]. Clarke, T. M.; Durrant, J. R. Charge Photogeneration in Organic Solar Cells. Chem. Rev. 2010, 110 (11), 6736−6767.
[7]. Liu, F.; Gu, Y.; Shen, X.; Ferdous, S.; Wang, H.-W.; Russell, T.P. Characterization of the morphology of solution-processed bulk heterojunction organic photovoltaics. Prog. Polym. Sci. 2013, 38,1990−2052.
[8]. Ye, L.; Zhang, S.; Ma, W.; Fan, B.; Guo, X.; Huang, Y.; Ade, H.; Hou, J. From Binary to Ternary Solvent: Morphology Fine−tuning of D/A Blends in PDPP3T-based Polymer Solar Cells. Adv. Mater. 2012, 24, 6335−6341.
[9]. Ye, L.; Jing, Y.; Guo, X.; Sun, H.; Zhang, S.; Zhang, M.; Huo, L.; Hou, J. Remove the Residual Additives toward Enhanced Efficiency with Higher Reproducibility in Polymer Solar Cells. J. Phys. Chem. C 2013, 117, 14920−14928
[10]. G. Dennler, M. C. Scharber and C. J. Brabec, Adv. Mater., 2009, **21**, 1323–1338.
[11]. J. Kalowekamo and E. Baker, Solar energy, 2009, **83**, 1224-1231.
[12]. M. Scharber, D. Muhlbacher, M. Koppe, P. Denk, C. Waldauf, A. J. Heeger and C. Brabec, Adv. Mater., 2006, **18**, 789-794.
[13]. K. M. Coakley and M. D. McGehee, Chem. Mater., 2004, **16**, 4533-4542.

[14]. J. Y. Kim, K. Lee, N. E. Coates, D. Moses, T. Q. Nguyen,M. Dante and A. J. Heeger, Science, 2007, **317**, 222–225.
[15]. Y. Liang, Z. Xu, J. B. Xia, S. T. Tsai, Y. Wu, G. Li, C. Ray and L.P. Yu, Adv. Mater., 2010, **22**, E135–E138.
[16]. H.-Y. Chen, J. Hou, S. Zhang, Y. Liang, G. Yang, Y. Yang, L. Yu, Y. Wu and G. Li, Nat. Photon., 2009, **3**, 649-653.
[17]. R. F. Service, Science, 5 2011, **332**, 293.
[18]. T. Chu, J. Lu, S. Beaupr, Y. Zhang, J. Pouliot, S. Wakim, J. Zhou, M. Leclerc, Z. Li, J. Ding and Y. Tao, J. Am. Chem. Soc., 2011,**133**, 4250-4253.
[19]. S. C. Price, A. C. Stuart, L. Yang, H. Zhou and W. You, J. Am. 10 Chem. Soc., 2011, **133**, 4625-4631.
[20]. H. Zhou, Y. Yang, A. C. Stuart, S. C. Price, S. Liu and W. You, Angew. Chem., Int. Ed., 2011, **50**, 2995.
[21]. Z. He, C. Zhong, X. Huang, W.-Y. Wong, H. Wu, L. Chen, S. Su, Y. Cao, Adv. Mater. 2011, **23**, 4636–4643
[22]. C. E. Small, S. Chen, J. Subbiah, C. M. Amb, S.-W. Tsang, T.-H. Lai, J. R. Reynolds and F. So, Nat. Photon., 2012, **6**, 115 120.
[23]. L. Dou, J. You, J. Yang, C.-C. Chen, Y. He, S. Murase, T. Moriarty, K. Emery, G. Li and Y. Yang, Nat. Photon., 2012, Accepted.
[24]. H Wang, Y. Liu, M. Li, H. Huang, H. M. Xu, R. J. Hong, and H. Shen, "Multifunctional TiO2 nanowires-modified nanoparticles bilayer film for 3D dye-sensitized solar cells," *Optoelectron. Adv. Mater. Rapid Commun.*, vol. 4, no. 207890, pp. 1166–1169, 2010.
[25]. Veldman A, Meskers SCJ, Janssen RAJ. The energy of charge-transfer states in electron donor–acceptor blends: insight into the energy losses in organic solar cells. Advanced Functional Materials2009;19:1939–48
[26]. M. C. Scharber and N. S. Sariciftci, "Efficiency of bulk-heterojunction organic solar cells.," *Prog. Polym. Sci.*, vol. 38, no. 12, pp. 1929–1940, Dec. 2013.
[27]. Kirchartz T, Taretto K, Rau U. Efficiency limits of organicbulk heterojunction solar cells. Journal of Physical Chemistry C2009;113:17958–66.
[28]. D. E. Markov, E. Amsterdam, P. W. M. Blom, A. B. Sieval and J.C. Hummelen, J. Phys. Chem. A, 2005, **109**, 5266-5274.
[29]. H. J. Son, F. He, B. Carsten and L. Yu, J. Mater. Chem., 2011, **21**, 18934-18945.
[30]. D. Gendron and M. Leclerc, Energy Environ. Sci., 2011, 4, 1225- 1237
[31]. Koster LJA, Shaheen SE, Hummelen JC. Pathways to a new effi-ciency regime for organic solar cells. Advanced Energy Materials2012;2:1246–53.
[32]. Gruber M, Wagner J, Klein K, Hörmann U, Opitz A,Stutzmann M, Brütting W. Thermodynamic efficiencylimit of molecular donor–acceptor solar cells and itsapplication to diindenoperylene/C60-based planar het-erojunction devices. Advanced Energy Materials 2012;2:1100–8.
[33]. Giebink NC, Wiederrecht GP, Wasielewski MR, Forrest SR. Thermo-dynamic efficiency limit of excitonic solar cells. Physical Review B2011;83, 195326/1–6.
[34]. Y. Zhou, M. Eck, M. Kruger, Bulk-heterojunction hybrid solar cells based on colloidal nanocrystals and conjugated polymers, Energy & Environmental Science 3 (2010) 1851–1864.
[35]. T. Xu, Q. Qiao, Conjugated polymer–inorganic semiconductor hybrid solar cells, Energy & Environmental Science 4 (2011) 2700–2720.
[36]. S. Ren, L.-Y. Chang, S.-K. Lim, J. Zhao, M. Smith, N. Zhao, V. Bulovic, M. Bawendi, S. Gradec˘ak, Inorganic–Organic hybrid solar cell: bridging quantum dots to conjugated polymer nanowires, Nano Letters 11 (2011) 3998–4002.
[37]. Y. Zhou, M. Eck, C. Veit, B. Zimmermann, F. Rauscher, P. Niyamakom, S. Yilmaz, I. Dumsch, S. Allard, U. Scherf, M. Kruger, Efficiency enhancement for bulk-heterojunction hybrid solar cells based on acid treated CdSe quantum dots and low Bandgap polymer PCPDTBT, Solar Energy Materials and Solar Cells 95 (2011) 1232–1237.
[38]. D. Celik, M. Krueger, C. Veit, H.F. Schleiermacher, B. Zimmermann, S. Allard, I. Dumsch, U. Scherf, F. Rauscher, P. Niyamakom, Performance enhancement of CdSe nanorod-polymer based hybrid solar cells utilizing a novel combi- nation of post-synthetic nanoparticle surface treatments, Solar Energy Materials and Solar Cells 98 (2012) 433–440.
[39]. S. Dayal, N. Kopidakis, D.C. Olson, D.S. Ginley, G. Rumbles, Photovoltaic devices with a low band Gap polymer and CdSe nanostructures exceeding 3% efficiency, Nano Letters 10 (2009) 239–242.
[40]. N.C. Nicolaidis, B.S. Routley, J.L. Holdsworth, W.J. Belcher, X. Zhou, P.C. Dastoor, Fullerene contribution to photocurrent generation in orga- nic photovoltaic cells, The Journal of Physical Chemistry C 115 (2011) 7801–7805.
[41]. J. Huang, Z. Huang, Y. Yang, H. Zhu, T. Lian, Multiple exciton dissociation in CdSe quantum dots by ultrafast electron transfer to adsorbed methylene blue, Journal of the American Chemical Society 132 (2010) 4858–4864.
[42]. M. Wright and A. Uddin, "Solar Energy Materials & Solar Cells Organic — inorganic hybrid solar cells : A comparative review," *Sol. Energy Mater. Sol. Cells*, vol. 107, pp. 87–111, 2012.

[43]. M.C.Scharber, DMühlbacher, M.Koppe ,P.Denk, C.Waldauf, A.J.Heeger, C.J. Brabec, Design rules for donors in bulk-Heterojunction solar cells— towards 10%energy- conversionefficiency,AdvancedMaterials18(2006) 789 794.
[44]. Vandewal, K., Gadisa, A., Oosterbaan, W. D., Bertho, S., Banishoeib, F., Van Severen, I., Lutsen, L., Cleij, T. J., Vanderzande, D. and Manca, J. V. (2008), The Relation Between Open-Circuit Voltage and the Onset of Photocurrent Generation by Charge-Transfer Absorption in Polymer : Fullerene Bulk Heterojunction Solar Cells. Adv. Funct. Mater., 18: 2064–2070.
[45]. V.D. Mihailetchi, H.X. Xie, B. de Boer, L.J.A. Koster, P.W.M. Blom, Charge Transport and photocurrent generation in poly(3-hexylthiophene): metha- nofullerene bulk-heterojunction solar cells, Advanced Functional Materials 16 (2006) 699–708.
[46]. W. Ma, C. Yang, X. Gong, K. Lee, A.J. Heeger, Thermally Stable, Efficient polymer solar cells with nanoscale control of the interpenetrating network morphology, Advanced Functional Materials 15 (2005) 1617–1622.
[47]. M.S. Ryu, H.J. Cha, J. Jang, Effects of thermal annealing of polymer:fullerene photovoltaic solar cells for high efficiency, Current Applied Physics 10 (2010) S206– S209
[48]. Huo, L. J.; Hou, J. H. Benzo[1,2-b:4,5-b′]dithiophene-based conjugated polymers: band gap and energy level control and their application in polymer solar cells. Polym. Chem. 2011, 2, 2453−2461.
[49]. Wang, M.; Hu, X. W.; Liu, P.; Li, W.; Gong, X.; Huang, F.; Cao, Y. Donor Acceptor Conjugated Polymer Based on Naphtho[1,2-c:5,6- c]bis[1,2,5]thiadiazole for High-Performance Polymer Solar Cells. J.Am. Chem. Soc. 2011, 133, 9638−9641. Am. Chem. Soc. 2011, 133, 9638−9641.
[50]. Price, S. C.; Stuart, A. C.; Yang, L.; Zhou, H.; You, W. Fluorine Substituted Conjugated Polymer of Medium Band Gap Yields 7% Efficiency in Polymer−Fullerene Solar Cells. J. Am. Chem. Soc. 2011,133, 4625−4631.
[51]. Li, K.; Li, Z.; Feng, K.; Xu, X.; Wang, L.; Peng, Q. Development of Large Band-Gap Conjugated Copolymers for Efficient Regular Single and Tandem Organic Solar Cells. J. Am. Chem. Soc. 2013, 135, 13549−13557.
[52]. Yang, T. B.; Wang, M.; Duan, C. H.; Hu, X. W.; Huang, L.; Peng, J. B.; Huang, F.; Gong, X. Inverted polymer solar cells with 8.4% efficiency by conjugated polyelectrolyte. Energy Environ. Sci. 2012, 5,8208−8214.

[53]. Zhang, M.; Guo, X.; Zhang, S.; Hou, J. Synergistic Effect of Fluorination on Molecular Energy Level Modulation in Highly Efficient Photovoltaic Polymers. Adv. Mater. 2014, 26, 1118−1123.
[54]. Cui, C.; Wong, W.-Y.; Li, Y. Improvement of Open-Circuit Voltage and Photovoltaic Properties of 2D-Conjugated Polymers by Alkylthio Substitution. Energy Environ. Sci. 2014, DOI: 10.1039/C4EE00446A.
[55]. Li, X. H.; Choy, W. C. H.; Huo, L. J.; Xie, F. X.; Sha, W. E. I.; Ding, B. F.; Guo, X.; Li, Y. F.; Hou, J. H.; You, J. B.; Yang, Y. Dual Plasmonic Nanostructures for High Performance Inverted Organic Solar Cells. Adv. Mater. 2012, 24, 3046−3052.
[56]. Liu, S.; Zhang, K.; Lu, J.; Zhang, J.; Yip, H.-L.; Huang, F.; Cao, Y. High-Efficiency Polymer Solar Cells via the Incorporation of an Amino-Functionalized Conjugated Metallopolymer as a Cathode Interlayer. J. Am. Chem. Soc. 2013, 135, 15326−15329.
[57]. Liao, S.-H.; Jhuo, H.-J.; Cheng, Y.-S.; Chen, S.-A. Fullerene Derivative-Doped Zinc Oxide Nanofilm as the Cathode of Inverted Polymer Solar Cells with Low-Bandgap Polymer (PTB7-Th) for High Performance. Adv. Mater. 2013, 25, 4766−4771.
[58]. Tan, Z. a.; Li, L.; Wang, F.; Xu, Q.; Li, S.; Sun, G.; Tu, X.; Hou, X.; Hou, J.; Li, Y. Solution-Processed Rhenium Oxide: A Versatile Anode Buffer Layer for High Performance Polymer Solar Cells with Enhanced Light Harvest. Adv. Energy Mater. 2014, DOI: 10.1002aenm.201300884
[59]. Cabanetos, C.; El Labban, A.; Bartelt, J. A.; Douglas, J. D.;Mateker, W. R.; Frechet, J. M. J.; McGehee, M. D.; Beaujuge, P. M. Linear Side Chains in Benzo[1,2-b:4,5-b′]dithiophene-Thieno[3,4- c]pyrrole-4,6-dione Polymers Direct Self-Assembly and Solar Cell Performance. J. Am. Chem. Soc. 2013, 135, 4656−4659.
[60]. Dou, L. T.; Chang, W. H.; Gao, J.; Chen, C. C.; You, J. B.; Yang, Y. A Selenium-Substituted Low-Bandgap Polymer with Versatile Photovoltaic Applications. Adv. Mater. 2013, 25, 825−831.
[61]. Dou, L. T.; Gao, J.; Richard, E.; You, J. B.; Chen, C. C.; Cha, K. C.; He, Y. J.; Li, G.; Yang, Y. Systematic Investigation of Benzodithiophene- and Diketopyrrolopyrrole-Based Low-Bandgap Polymers Designed for Single Junction and Tandem Polymer Solar Cells. J. Am. Chem. Soc. 2012, 134, 10071−10079.
[62]. Huo, L. J.; Zhang, S. Q.; Guo, X.; Xu, F.; Li, Y. F.; Hou, J. H. Replacing Alkoxy Groups with Alkylthienyl Groups: A Feasible Approach To Improve the Properties of Photovoltaic Polymers. Angew. Chem., Int. Ed. 2011, 50, 9697−9702.
[63]. Duan, R. M.; Ye, L.; Guo, X.; Huang, Y.; Wang, P.; Zhang, S. Q.; Zhang, J. P.; Huo, L. J.; Hou, J. H. Application of Two-Dimensional Conjugated Benzo[1,2-b:4,5-b′]dithiophene in Quinoxaline-Based Photovoltaic Polymers. Macromolecules 2012, 45, 3032−3038.
[64]. Zhang, S.; Ye, L.; Wang, Q.; Li, Z.; Guo, X.; Huo, L.; Fan, H.; Hou, J. Enhanced Photovoltaic Performance of Diketopyrrolopyrrole (DPP)-Based Polymers with Extended π Conjugation. J. Phys. Chem. C 2013, 117, 9550−9557.
[65]. Huo, L. J.; Hou, J. H.; Zhang, S. Q.; Chen, H. Y.; Yang, Y. A Polybenzo[1,2-b:4,5-b′]dithiophene Derivative with Deep HOMO Level and Its Application in High-Performance Polymer Solar Cells. Angew. Chem., Int. Ed. 2010, 49, 1500−1503
[66]. Dong, Y.; Hu, X.; Duan, C.; Liu, P.; Liu, S.; Lan, L.; Chen, D.; Ying, L.; Su, S.; Gong, X.; Huang, F.; Cao, Y. A Series of New Medium-Bandgap Conjugated Polymers Based on Naphtho[1,2-c:5,6- c]bis(2-octyl-[1,2,3]triazole) for High-Performance Polymer Solar Cells. Adv. Mater. 2013, 25, 3683−3688
[67]. Zuo, G.; Li, Z.; Zhang, M.; Guo, X.; Wu, Y.; Zhang, S.; Peng, B.; Wei, W.; Hou, J. Influence of the backbone conformation of conjugated polymers on morphology and photovoltaic properties. Polym. Chem. 2014, 5, 1976−1981.
[68]. Guo, X.; Zhang, M.; Huo, L.; Xu, F.; Wu, Y.; Hou, J. Design, synthesis and photovoltaic properties of a new D-π-A polymer with extended π-bridge units. J. Mater. Chem. 2012, 22, 21024−21031.
[69]. Huang, Y.; Guo, X.; Liu, F.; Huo, L. J.; Chen, Y. N.; Russell, T. P.; Han, C. C.; Li, Y. F.; Hou, J. H. Improving the Ordering and Photovoltaic Properties by Extending pi-Conjugated Area of Electron-Donating Units in Polymers with D-A Structure. Adv. Mater. 2012, 24,3383−3389.
[70]. Wu, Y.; Li, Z.; Ma, W.; Huang, Y.; Huo, L.; Guo, X.; Zhang, M.; Ade, H.; Hou, J. PDT-S-T: A New Polymer with Optimized Molecular Conformation for Controlled Aggregation and π−π Stacking and Its Application in Efficient Photovoltaic Devices. Adv. Mater. 2013, 25, 3449−3455.
[71]. L. Ye, S. Zhang, L. Huo, M. Zhang, and J. Hou, "Molecular design toward highly efficient photovoltaic polymers based on two-dimensional conjugated benzodithiophene," *Acc. Chem. Res.*, vol. 47, pp. 1595–1603, 2014.
[72]. Xie, L.-H.; Yin, C.-R.; Lai, W.-Y.; Fan, Q.-L.; Huang, W. Prog. Poly. Sci. **2012**, 37, 1192.
[73]. McCulloch, I.; Ashraf, R. S.; Biniek, L.; Bronstein, H.; Combe, C.; Donaghey, J. E.; James, D. I.; Nielsen, C. B.; Schroeder, B. C.; Zhang, W. M. Acc. Chem. Res. **2012**, 45, 714
[74]. H. Zhong, Z. Li, F. Deledalle, E. C. Fregoso, M. Shahid, C. B. Nielsen, N. Yaacobi-gross, S. Rossbauer, T. D. Anthopoulos, J. R. Durrant, and M. Heeney, "Fused Dithienogermolodithiophene low band gap polymers for high performance organic solar cells without processing additives."
[75]. Cardona, C. M.; Li, W.; Kaifer, A. E.; Stockdale, D.; Bazan, G. C. Adv. Mater. **2011**, 23, 2367
[76]. L. Dou, W. Chang, J. Gao, C. Chen, J. You, and Y. Yang, "COMMUNICATION A Selenium-Substituted Low-Bandgap Polymer with Versatile Photovoltaic Applications," pp. 1–7
[77]. A. J. Kronemeijier , E. Gili , M. Shahid , J. Pivnay , A. Salleo , M. Heeney , H. Sirringhaus , Adv. Mater. **2012** , 24 , 1558 ;
[78]. J. S. Ha , K. H. Kim , D. H. Choi , J. Am. Chem. Soc. **2011** , 133 , 10364 ; c) M. Shahid , T. Mccarthy-Ward , J. Labram , S. Rossbauer , E. B. Domingo , S. E. Watkins , N. Stingelin , T. D. Anthopoulos , M. Heeney , Chem. Sci. **2012** , 3 , 181